J Biol Phys (2015) 41:293–301
DOI 10.1007/s10867-015-9379-y

ORIGINAL PAPER

Far-infrared spectroscopy of salt penetration into a collagen fiber scaffold

Maya Mizuno · Akira Yamada · Kaori Fukunaga · Hiroaki Kojima

Received: 19 August 2014 / Accepted: 19 January 2015 / Published online: 13 March 2015

Abstract We employed far-infrared spectroscopy to observe the amount of salt that penetrates into collagen fiber masses. The absorption properties of collagen sheets prepared from tilapia skin, bovine skin, rat tail, and sea cucumber dermis were measured using a transmission Fourier transform spectrometer in a band from approximately 100 to 700 cm^{-1}. We confirmed that the absorbance spectra of the four types of dried collagen sheet show good agreement, even though the amino acid compositions differed. The absorbance peaks observed in the band corresponded to collective vibrations of plural functional groups such as methylene and imino groups in collagen. When salt solution was added to the collagen sheets and then dried, the spectral shapes of the sheets at approximately 166 cm^{-1} were clearly different from those of the plain collagen sheets. The differential absorbance between wavenumbers 166 cm^{-1} and 250 cm^{-1} sensitively reflected the difference between higher-order structures, and the salt diffusion (crystallization) depended on the collagen fiber condition. From these results, we consider that spectral changes can be used for the numerical evaluation of salt penetration into a collagen fiber scaffold.

Keywords Collagen fiber · Salt · Penetration · Absorbance spectrum

1 Introduction

Collagen is present in tissues such as the cornea, dermis, and bone, and is typically used as a scaffold in organ growth and tissue engineering. The structure of collagen affects the behavior

M. Mizuno · K. Fukunaga
Applied Electromagnetic Research Institute, National Institute of Information and Communications Technology, 4-2-1 Nukui-kitamachi, Koganei, Tokyo 184-8795, Japan

A. Yamada · H. Kojima
Advanced ICT Research Institute, National Institute of Information and Communications Technology, 588-2 Iwaoka, Kobe 651-2492, Japan

M. Mizuno (✉)
Electromagnetic Compatibility Laboratory, Applied Electromagnetic Research Institute, National Institute of Information and Communications Technology, 4-2-1 Nukui-kitamachi, Koganei, Tokyo 184-8795, Japan
e-mail: mmizuno@nict.go.jp

of generated tissues and cells, and can promote successful adaptations, leading to enhanced expressions of cell-specific morphologies and functions. The structure of collagen must be studied so that scaffolds composed of collagen can be optimized. The analysis of the structures and molecular behavior of collagen are carried out by various methods such as nuclear magnetic resonance (NMR) analysis, X-ray diffraction (XRD) analysis, and Raman and Fourier transform infrared (FT-IR) spectroscopy [1–3]. These techniques were developed a long time ago, and new measurement methods such as stable isotope labeling for NMR analysis and single protein crystals for XRD analysis have been developed since then. In such studies, spectral changes caused by hydration, the presence of salt, and denaturation were observed [4–7].

On the other hand, far-infrared (or terahertz) spectroscopic studies of proteins have expanded since the 1960s [8–10], and they have accelerated with the development of the terahertz time-domain spectrometer [11] in the 1990s. Many absorption peaks in proteins have been observed and assignment to each vibrational motion has been attempted. Large molecules such as collagen generally have a broad absorption band, whereas spectra are markedly affected by electrostatic interactions from ions and other molecules. On the basis of the sensitivity against electrostatic interactions in composites, we believe that the evaluation of salt penetration into a collagen scaffold material can be more easily and numerically investigated in relation to the evaluation of efficiency of absorption of nutrition (such as Na^+) from the medium in three-dimensional cell culture.

In this study, we verified the absorption properties of plain collagen fiber sheets and whether changes in the absorbance spectra of dried collagen fiber sheets clearly depend on the distribution of salt crystals inside collagen fiber masses. The results suggest the penetrability of salt solution in the collagen scaffolds used for tissue engineering.

2 Measurement specimens and method

Dried collagen sheets were prepared from the bovine skin, tilapia skin, rat tail, and sea cucumber dermis. We bought oriented cross-linked type I collagen sheets manufactured from bovine skin, tilapia skin, and rat tail by Atree Inc. The thickness of the three samples was approximately 23 μm. In the case of the sea cucumber dermis, we adjusted the collagen suspension of approximately 5.9 wt% [12]. Aliquots (1.7 mg) of the sea cucumber collagen were formed into disks (4 mm in diameter) on a cyclo-olefin polymer plate and naturally dried at 27 °C. To produce disks with different internal conditions, some of the dried collagen samples were soaked in 3 ml of phosphate-buffered saline (PBS) of different concentrations, or the collagen suspensions were heated to 50 °C and soaked in 3 ml of 6×PBS, and then dried at a temperature of 25–26 °C and a relative humidity of 34–36% before the absorbance spectra were measured. In the heat treatment, we used a temperature controller (ThermoPlate, Tokai Hit Co., Ltd.) and placed a sample between the controller plate and the cyclo-olefin polymer plate. The thickness of the sea cucumber collagen samples was approximately 20 μm.

A Fourier transform spectrometer (VIR-F; JASCO) with a ceramic lamp was mainly used to obtain the absorbance spectra of the collagen samples between 100 and 700 cm^{-1}. To verify the absorbance spectra at low frequencies (approximately from 30 to 100 cm^{-1}), a terahertz time-domain spectrometer (Rayfact SpecTera RS-01020, Tochigi Nikon) was used.

We compared the measured and calculated spectral shapes for a collagen model peptide. The semi-empirical quantum chemistry software Molecular Orbital Package (MOPAC) 2012 based on the neglect of diatomic differential overlap approximation was used with a Parameterized Model number 7 (PM7) Hamiltonian containing diffuse function [13, 14]. The spectral

band half width and wavenumber resolution were set to 50 cm^{-1} and 5 cm^{-1}, respectively, in the calculation. The molecular model structure was optimized by the eigenvector following (EF) method. Molecular vibrational directions and infrared absorption spectra were visualized using Facio software [15].

3 Results and discussion

We measured the absorption spectrum of a plain collagen sheet prepared from tilapia skin, in the range from 1 to 700 cm^{-1} at approximately 27 °C. We found three broad absorption bands at approximately 130, 340, and 600 cm^{-1}. As shown in Fig. 1, the absorption bands are almost in agreement with those of a quantum chemistry calculation (MOPAC 2012) using a collagen peptide model, $(Gly–Pro–Hyp–Gly–Pro–Hyp–Gly–Ala–Hyp–Gly–Pro–Hyp)_3$. Two absorption peaks calculated at 560 and 670 cm^{-1} could not be clearly split in the measurement owing to the broadness of the absorption band influenced by vibrational damping. When we used a previous parameterization (PM6) for the quantum chemistry calculation, the peak frequencies shifted to a lower frequency with a shift amount of 20 cm^{-1} or more. We considered that the shift was caused by the difference in the basis set, and the addition of a diffuse function to the basis set was required for comparison, particularly in the low-frequency range. The observed molecular vibrational directions, shown in Fig. 1 by arrowheads, indicated that vibrations of the collagen model in the band corresponded to the collective vibration of plural functional groups such as methylene, imino, and carbonyl groups. The main functional groups that vibrated in the collagen model peptide differed depending on the frequency. For example, we were able to observe bending vibrations of methylene groups (rocking) and imino groups (in-plane) at 564.1 cm^{-1}. However, we were unable to clearly assign them to such vibrational modes in the low-frequency range. The backbone of the collagen hardly moved in the range from 1 to 700 cm^{-1}.

To verify the spectral dependence on the amino acid composition and the combination of polypeptide chains, we compared the absorption spectra of the naturally dried collagen sheets

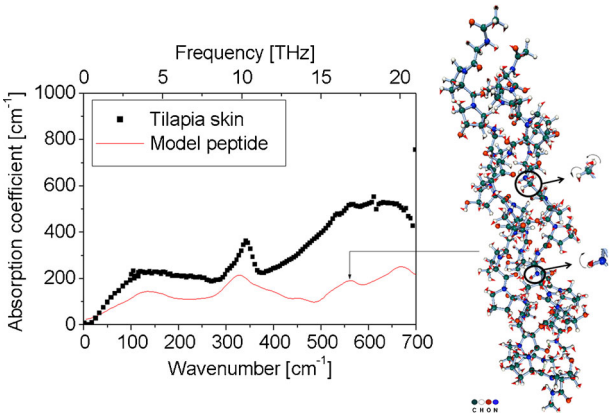

Fig. 1 Absorption spectral comparison between result of simulation using semi-empirical quantum chemistry software (MOPAC 2012) and result of measurement of a collagen fiber sheet made from tilapia skin (*left figure*). In the simulation, a collagen peptide model, $(Gly–Pro–Hyp–Gly–Pro–Hyp–Gly–Ala–Hyp–Gly–Pro–Hyp)_3$, with a triple helical structure was used. *Arrowheads* in the *right figure* show molecular vibrational direction at 564.1 cm^{-1}

made from tilapia skin, bovine skin, rat tail, and sea cucumber dermis. The absorption coefficient was calculated from the measured absorbance. Figure 2 shows that the spectral shapes of the four types of collagen are in good agreement, even though the amino acid compositions and the numbers of amino acids are different [16–18]. In addition, three helical chains of the sea cucumber collagen showed the same components; the combination of polypeptide chains was different from that of collagen type I [19]. These findings indicate that many different types of collagen have a similar absorption spectral shape. Collagen commonly consists mainly of glycine and includes functional groups such as imino and carbonyl groups. We therefore postulated that the absorption properties from 100 to 700 cm^{-1} are mainly related to the vibration of glycine or common functional groups. From the quantum chemistry calculation mentioned above, the latter would be more discernible in absorption spectra. The spectral shapes of the collagens were similar to those of other peptides such as AK17 and AK10G having a helical structure [20]. AK17 is a 17-amino-acid alanine-rich peptide containing three lysine residues. AK10G differs from AK17 in the glycine substitution at the 10th position. Because the main component of the peptides was not glycine, it may be reasonable to consider that the absorption properties are mainly related to the vibration of common functional groups.

Next, we measured the absorbance of collagen sheets containing salts and examined whether the absorbance spectral changes depend on the salt concentration. We measured the spectra of the naturally dried sea cucumber collagen sheets after they had been soaked in 3 ml of PBS at seven concentrations of zero, one, two, four, six, eight, and ten times the original concentration. Adding salt to the collagen samples caused the spectral shape to change noticeably at low frequencies (Fig. 3). Here, the spectra were normalized at 368 cm^{-1} for apparent comparison at the different salt concentrations used. Absorption peaks were observed at approximately 166 and 340 cm^{-1}, and only the magnitude of the peak at approximately 166 cm^{-1} changed with the salt concentration. The presence of salts caused the absorbance at approximately 166 cm^{-1} to increase until the PBS concentration reached six times the original concentration. High concentration conditions were hardly analyzable owing to contraction of collagen samples. We therefore used 6×PBS as a biological marker to distinguish the conditions of the collagen samples for the next measurements. In addition, when we added saline to a collagen sheet, we found that the collagen sample showed a peak nearly equal to that of 1×PBS containing other salts such as KH_2PO_4 and Na_2HPO_4. We therefore considered

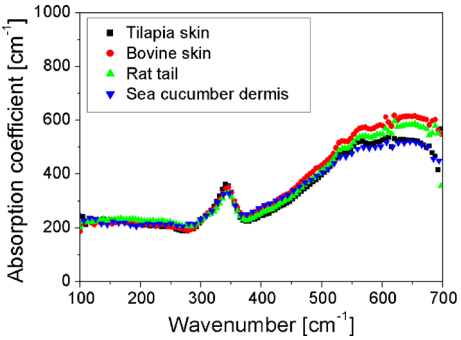

Fig. 2 Absorption spectra of collagen fiber sheets prepared from tilapia skin, bovine skin, rat tail, and sea cucumber dermis. The spectral shapes of the four types of collagen are in good agreement, even though the amino acid compositions are different. Two broad absorption bands at approximately 340 and 600 cm^{-1} were found

that the observed absorption was mainly related to Na^+ and Cl^- with collagen. Here, note that the spectrum of vacuum-dried salt powder with particle size less than 25 μm showed a small broad absorption peak for sodium chloride crystals [21], as seen in the inset of Fig. 3. However, the magnitude of the absorbance was smaller than that of salts with collagen and was similar between 250 cm^{-1} and 166 cm^{-1} when the sample component was only PBS (Fig. 3 inset). Thus, we considered that the magnitude of the absorbance depends on the electrostatic interaction between collagen and salts and that it is better to analyze the differential absorbance (ΔAbs) shown in Fig. 3 so that we can eliminate the absorbance caused by only the salt crystals.

To determine the source of the absorption peak at approximately 166 cm^{-1}, we heated a sea cucumber collagen suspension to 50 °C to change higher-order structures by denaturation. The denaturation temperature is approximately 33 °C [22]. We measured the absorbance spectra of the sea cucumber collagen sheets which were naturally dried at 25–26 °C after the collagen suspensions were heated and then soaked in 3 ml of 6×PBS. Figure 4 shows the heating time dependence of ΔAbs from 0 to 10 min. Each ΔAbs is the mean of three samples, and error bars indicate standard deviations (±1σ). ΔAbs decreased with an increase in heating time owing to a large increase in the absorbance at 250 cm^{-1} and a slight change in that at 166 cm^{-1} (Fig. 4 inset). We inferred that the changes in absorption reflected changes in the conformation of the dried collagen and salts caused by the difference in the electrostatic interaction between the collagen and salts before drying. We calculated the dipole moment and vibrational modes of a single-chain peptide model in the presence of sodium and chloride ions to confirm single-chain behavior at both ends of the heated collagen. The dipole moment direction of the single chain with the crystal was close to being vertical against the main chain, whereas the magnitude was smaller than one-third of that of the triple chain. As shown in Fig. 5, the absorption spectral shape of the single-chain peptide with the ions was similar to those in Fig. 3. Strong absorption appeared only when structure optimization was carried out in the presence of both the single-chain peptide and the ions. We found some vibrational motion related to both the ions and the single-chain peptide from 100 to 200 cm^{-1}. The collective vibration has a large movement only around the ions, and the backbone also moved, for example, at 162.9 cm^{-1} (Fig. 6). We therefore inferred that a new absorption peak appeared because of the

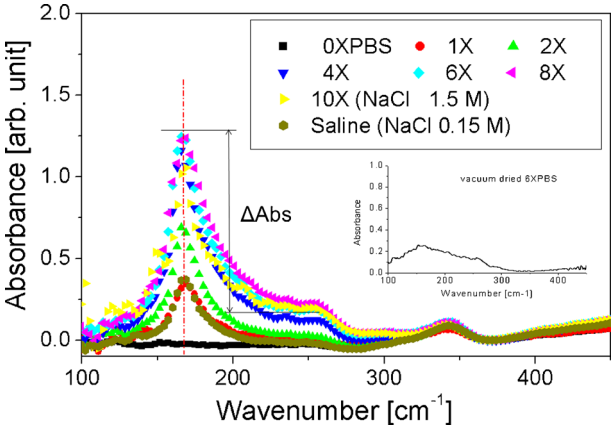

Fig. 3 Spectral dependences of the collagen sample on the concentration of salt in phosphate-buffered saline (PBS). Here, sea cucumber collagen was used. For comparison, the spectrum of the collagen with salt added without phosphate is also indicated. Moreover, the spectrum of vacuum-dried 6×PBS (3 ml) is shown in the inset

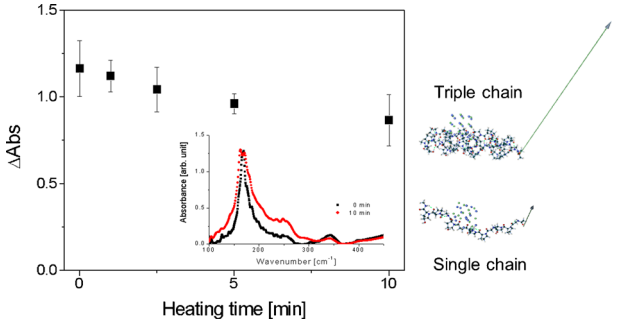

Fig. 4 Differential absorbance changes of sea cucumber collagen sample heated to 50 °C for 0 to 10 min (*left figure*). Each indicated value is the mean of three samples, and *error bars* are standard deviations (±1σ). Absorbance spectra of the samples heated for 0 and 10 min are shown in the inset. Simulated schematic representations of dipole moment are also indicated with *arrows* for the single- and triple-chain model peptide with NaCl (*right figure*)

instability of the salt and collagen structure, and the triple chain with the crystal also has similar vibrational properties. Furthermore, it is assumed that the magnitude changes were caused by the increase in the length of the single chain in the heated sample. The high-order structure must be understood before the observation of salt penetration. Absorbance changes dependent on denaturation could be observed by various methods such as circular dichroism.

Finally, we attempted to detect the difference in salt penetration among the sea cucumber collagen sheets using ΔAbs. We prepared samples with and without mixing with PBS. The samples with mixing were uniformly dispersed in 6×PBS and then dried, whereas 6×PBS was added to the samples without mixing after drying the plain sheet for over 25 h to repel PBS via hydrophobic bonding. From Fig. 7, we confirmed that ΔAbs and its variation for the sample mixed with PBS were larger than those of the sample with PBS added without mixing. Each ΔAbs is the mean of three samples, and error bars indicate standard deviations (±1σ). We considered that the difference was caused by the difference in the electrostatic interaction between the collagen and salts because the absorbance spectra were mainly different in terms of their magnitude at 166 cm^{-1}, as shown in the inset of Fig. 7. We examined salt crystals in the collagen samples under an optical microscope at a magnification of 100× (Fig. 7 inset). In the case of the PBS-mixed sample, the salts were present over the entire area and the salt

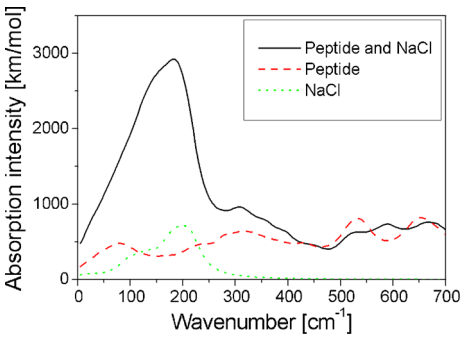

Fig. 5 Absorption spectra of single-chain model peptide with NaCl, only peptide, and NaCl using semi-empirical quantum chemistry software (MOPAC 2012). In the simulation, a peptide model, Gly–Pro–Hyp–Gly–Pro–Hyp–Gly–Ala–Hyp–Gly–Pro–Hyp, with a helical structure was used

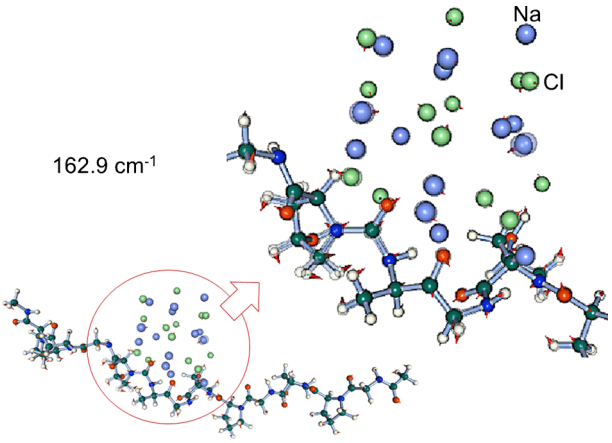

Fig. 6 Simulated schematic representations of molecular motion at 162.9 cm^{-1} in single-chain peptide model with NaCl optimized from crystal lattice model. The *circle* emphasizes the position of the large molecular motion. Here, two images were overlapped. The overlapped images show that the molecule and ions are in motion

crystals were small, indicating a high penetrability for this test scaffold. The sample with PBS added had inhomogeneous large salt crystals on the sample surface, indicating low penetrability. These findings indicate that the absorbance is related to the area of attachment between the ions and the collagen fiber. Far-infrared spectroscopy provides a means of evaluating the diffusion of salts inside collagen fiber masses. In the opinion of the authors, crystal formation is affected by various parameters such as the drying conditions (temperature and humidity), impurities, and collagen content. However, by controlling these parameters, this method would be useful for evaluating the dependence of salt penetration on the difference in surface hydrophobicity of the collagen scaffold material.

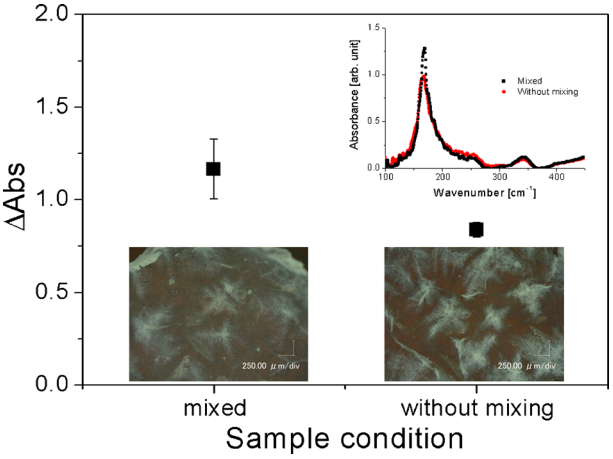

Fig. 7 Variation in differential absorbance of the samples with different salt conditions. Three samples mixed with PBS and three samples with PBS added without mixing were measured. Each indicated value is the mean of three samples, and *error bars* are standard deviations (±1σ). Examples of microscopy images showing sample surfaces and absorption spectra are shown in the *inset*

4 Conclusions

We prepared four types of dried collagen sheet from tilapia skin, bovine skin, rat tail, and sea cucumber dermis, and measured their absorbance spectra in the far infrared region. Their absorbance spectra are in good agreement. However, they clearly differed when the salts were added to collagen sheets. On the basis of the measured and calculated absorption properties, it was shown that the differential absorbance between wavenumbers 166 cm^{-1} and 250 cm^{-1} depended on the presence of high-order structures (single or triple chains) and the concentration of salt crystals inside the collagen sample. We, therefore, concluded that the presence of salts can be observed in collagen sheets using differential absorbance.

References

1. Mayo, K.H.: NMR and X-ray studies of collagen model peptides. Biopolymers (Pept. Sci) **40**, 359–370 (1996)
2. Gullekson, C., Lucas, L., Hewitt, K., Kreplak, L.: Surface-sensitive Raman spectroscopy of collagen I fibrils. Biophys. J. **100**, 1837–1845 (2011)
3. Vidal, B.C., Mello, M.L.: Collagen type I amide I band infrared spectroscopy. Micron **42**, 283–289 (2011)
4. Berendsen, H.J.C.: Nuclear magnetic resonance study of collagen hydration. J. Chem. Phys. **36**, 3297–3305 (1962)
5. Fung, B.M., Trautmann, P.: Deuterium NMR and EPR of hydrated collagen fibers in the presence of salts. Biopolymers **10**, 391–397 (1971)
6. Freudenberg, U., Behrens, S.H., Welzel, P.B., Müller, M., Grimmer, M., Salchert, K., Taeger, T., Schmidt, K., Pompe, W., Werner, C.: Electrostatic interactions modulate the conformation of collagen I. Biophys. J. **92**, 2108–2119 (2007)
7. Brown, E.M.: Effects of neutral salts on collagen structure and chromium–collagen interactions. J. Am. Leather Chem. Assoc. **94**, 59–67 (1999)
8. Falconer, R.J., Markelz, A.G.: Terahertz spectroscopic analysis of peptides and proteins. J. Infrared Milli. Terahz. Waves. **33**, 973–988 (2012)
9. Markelz, A.G., Roitberg, A., Heilweil, E.J.: Pulsed terahertz spectroscopy of DNA, bovine serum albumin and collagen between 0.1 and 2.0 THz. Chem. Phys. Lett. **320**, 42–48 (2000)
10. Acbas, G., Niessen, K.A., Snell, E.H., Markelz, A.G.: Optical measurements of long-range protein vibrations. Nat. Commun. **5**, 3076 (2014)
11. Sakai, K. (ed.): Terahertz optoelectronics. Topics Appl. Phys. **97**: 203 –271, Springer-Verlag, Berlin (2005)
12. Tamori, M., Yamada, A., Nishida, N., Motobayashi, Y., Oiwa, K., Motokawa, T.: Tensilin-like stiffening protein from *Holothuria leucospilota* does not induce the stiffest state of catch connective tissue. J. Exp. Biol. **209**, 1594–1602 (2006)
13. Stewart, J. J. P.: MOPAC2012. Stewart Computational Chemistry, Colorado Springs, CO, USA, HTTP://OpenMOPAC.net (2012)
14. Stewart, J.J.P.: Optimization of parameters for semiempirical methods VI: more modifications to the NDDO approximations and re-optimization of parameters. J. Mol. Model. **19**, 1–32 (2013)
15. Suenaga, M.: Development of GUI for GAMESS / FMO Calculation. J. Comput. Chem. Jpn. **7**, 33–54 (2008)
16. Potaros, T., Raksakulthai, N., Runglerdkreangkrai, J., Worawattanamateekul, W.: Characteristics of collagen from Nile tilapia (*Oreochromis niloticus*) skin isolated by two different methods. Kasetsart J. (Nat. Sci.) **43**, 584–593 (2009)
17. Mayne, J., Robinson, J.J.: Comparative analysis of the structure and thermal stability of sea urchin peristome and rat tail tendon collagen. J. Cell. Biochem. **84**, 567–574 (2002)
18. De Moor, S., Waite, J.H., Jangoux, M., Flammang, P.: Characterization of the adhesive from cuvierian tubules of the sea cucumber Holothuria forskali (Echinodermata, Holothuroidea). Mar. Biotechnol. **5**, 45–57 (2003)
19. Adibzadeh, N., Aminzadeh, S., Jamili, S., Karkhane, A.A., Farrokhi, N.: Purification and characterization of pepsin-solubilized collagen from skin of sea cucumber Holothuria parva. Appl. Biochem. Biotechnol. **173**, 143–154 (2014)

20. Ding, T., Huber, T., Middelberg, A.P.J., Falconer, R.J.: Characterization of low-frequency modes in aqueous peptides using far-infrared spectroscopy and molecular dynamics simulation. J. Phys. Chem. A **115**, 11559–11565 (2011)
21. Martin, T.P.: Interaction of finite NaC1 crystals with infrared radiation. Phys. Rev. B **1**, 3480–3488 (1970)
22. Liu, Z., Oliveira, A.C.M., Su, Y.C.: Purification and characterization of pepsin-solubilized collagen from skin and connective tissue of giant Red Sea cucumber (*Parastichopus californicus*). J. Agric. Food Chem. **58**, 1270–1274 (2010)